Theoretical Studies on Hydrogen Bonding Interactions: From Small Clusters to the Liquid Phase

ROBERTO RIVELINO

Instituto de Física, Universidade Federal da Bahia, 40210-340 Salvador, BA, Brazil

ABSTRACT: This article discusses some methodological aspects and applications of hydrogen bonding interactions in molecular aggregates, as well as in liquids, that have currently been considered in the literature. First, the concept of a hydrogen bond is revisited from the classic picture of a H-bonded pair of molecules. Second, an analysis of the interaction energy into various physically meaningful terms is presented within the quantum mechanical scope and applied for different H-bonded complexes. Third, cooperative effects are quantitatively considered in terms of electronic redistribution upon complexation. Fourth, some results are reviewed and new insights into the fundamental nature of the hydrogen bonding interaction are reported. Finally, the fundamental forces responsible for the formation of hydrogen bonds in condensed phase are examined by means of atomistic simulations based on classical force fields. © 2010 Wiley Periodicals, Inc. Int J Quantum Chem 111: 1256–1269, 2011

Key words: H-bond; cooperative effect; liquid

1. Introduction

S tudies of intermolecular interactions have been part of the research interests of Professor Sylvio Canuto during many years [1–4]. Among these studies, hydrogen bonding interactions have gained especial attention because of their importance in physical chemistry and biological systems [5–15]. On the quantum chemistry perspective, systematic studies of the methodological dependence of computed properties of H-bonded systems have also been carried out in Canutos's group [10, 11, 16–19]. Moreover, computational methods to investigate specific interactions between the solute and solvent in the liquid phase have been developed by Canuto, Coutinho, and coworkers [6, 8, 13, 15, 20–28]. Since then, he

has guided many PhD students in the direction of understanding properties and mechanisms in molecular aggregates and liquids [29]. In this sense, this article revisits important topics about hydrogen bonding interactions that have been subject of continuous interest of Professor Canuto and his collaborators [30–33]. Furthermore, new insights into the fundamental nature of the H-bonds in molecular complexes are presented [34, 35].

There have been important papers and reviews written about hydrogen bonding in molecular clusters and condensed phase over the years [36–40]. They have mainly allowed a detailed understanding of structural, binding, and vibrational properties of diverse H-bonded systems within the Born-Oppehheimer approximation. This knowledge has also been extended to design self-assembling materials through the interaction of H-bonds in the nanoscale [41–43]. From the electronic structure standpoint, density functional theory (DFT) methods have dramatically enhanced the level of accuracy that is expected from the calculations. Thus, taking an accurate electronic structure description into account, one obtains state-of-the-art information concerning the hydrogen bonding phenomenon in extended molecular systems.

On the other hand, for pure liquids and solutions, a fully quantum mechanical description is still complicated [44, 45], mainly because of the huge computational cost involving a large number of explicit molecules in these types of systems. Additionally, in the liquid phase, beyond the larger number of molecules considered, it is necessary to account for their numerous configurations. In this way, the use of a classic description of the system can reduce the cost of the calculations. This can be achieved through hybrid or sequential protocols. In a hybrid scheme, the classical and quantum mechanic regions are interfaced directly [46, 47], whereas in the sequential approach, a simulation of the liquid is used to generate structures that are then used in subsequent quantum mechanics calculations [20–28, 48]. In the latter procedure, pioneered by Canuto and Coutinho [6, 8, 13, 15, 20–28], a number of uncorrelated configurations of the liquid are selected from a Monte Carlo simulation, using the autocorrelation function of the energy [49]. Therefore, the focus converges on the separation of the intrinsic properties of the system under study (e.g., a solute) from the disturbances undergone by interactions with the binding moieties or solvent medium.

In the following sections, it is presented some definitions, methodologies, and results that

accompany the formation of a H-bond, in the electronic ground state and considering a closed shell system. The impact of H-bonding on the geometry, energetics, electronic redistributions, and spectroscopic properties is examined. These studies are based on many-body perturbation/coupled-cluster theories (MBPT/CC), and DFT calculations. Moreover, results on the simulation of hydrogen bonding in solutions are presented in terms of empirical potentials. The paper is concluded with new insights into the fundamental nature of the hydrogen bonding interaction and by throwing some light on the understanding of H-bonded molecular nanostructures in solutions [50, 51].

2. Theory and Calculations

A hydrogen bonding interaction is classically drawn as X—H···Y, where a hydrogen atom (H), covalently bound to a more electronegative atom (X), interacts with a region of high electron density (Y). Weaker than a conventional covalent bond, the H-bond is stronger than van der Waals interactions that bind together nonpolar molecules. Strictly speaking, X can be an atom like O, F, or N, whereas Y can be any σ or π electron donor site (e.g., a Lewis base) in the same or separate molecule [52–54]. Recently, metal atom gold has been proposed as a nonconventional proton acceptor [55]. Many authors have also given attention to less usual H-bonding interactions [56–58], wherein the donor X—H group does not necessarily involve atom X much more electronegative than H. In this case, the C—H donor has been shown to participate in H-bonds of surprising strength [56, 58].

There are important perturbations that accompany a H-bond formation [52]. However, two features are commonly accepted to all types of H-bonds: (i) there is a significant electronic redistribution from the proton acceptor (Y) to the proton donor (X—H); (ii) formation of the X—H···Y H-bond results in weakening of the X—H covalent bond. Usually, (ii) is accompanied by a bond elongation and concomitant decrease of the X—H stretch vibration frequency (red shift) compared with the isolated moieties. Also, a blue shift is sometimes expected to occur during the H-bond formation [59]. Computational advances in ab initio approaches have permitted a detailed

characterization of the hydrogen bonding phenomena in a variety of systems.

2.1. BINDING AND ZERO-POINT VIBRATONAL ENERGIES

The most common quantity calculated from ab initio calculations for a H-bonded system is the binding energy associated to the reaction X—H + Y → X—H···Y. The complexation energy of this process is taken as ΔE, which is defined as follows:

$$\Delta E = E(X - H \cdots Y) - [E(X - H) - E(Y)] \quad (1)$$

If a H-bonded complex is formed, then this is more stable than the isolated species and ΔE is negative; in other words, the binding energy is positive. As usual, all species are taken in their fully optimized geometries. Hence, changes in the internal geometries of both X—H and Y can lead to significant nuclear relaxation after the H-bond formation [54].

To calculate the strength of the H-bonding interaction, it is important to employ size-consistent correlated methods [60] such as the second-order Møller-Plesset (MP2) level of perturbation theory [61]. After obtaining the equilibrium structure, single-point calculations can be performed within the many-body perturbation/coupled-cluster theories (MBPT/CC). In this way, we are able to analyze the effects of high-order electron correlation in assembling the complex from its isolated moieties. As an alternative approach to compute the structure and energy of H-bonded complexes, DFT [35, 62, 63] has provided accurate results with lower computational cost than MBPT/CC. Usually, the performance of DFT methods depends on the basis set chosen, as well as the exchange-correlation functional employed in the calculations.

Currently, the use of large Gaussian-type basis sets, combined with correlated methods, has permitted to compute accurate properties of many H-bonded systems. For example, in the case of small clusters, such as H-bonded pairs of molecules, split-valence basis sets, augmented with polarization and diffuse functions [64, 65] (e.g., 6-311++G(d,p)) appears to be important basis sets required for reliable results. Also, in calculations that include electron correlation, the series of correlation-consistent polarized split-valence basis sets (cc-pVXZ, X = D, T, Q, 5, and 6)[66, 67] is entirely feasible. These basis sets can also be systematically employed with augmented and dif-

fuse functions (aug-cc-pVXZ), which are well suited for convergence studies [68]. Whereas large basis sets may improve the computations, the finite size introduces a nonphysical stabilization given by the basis set superposition error (BSSE). Thus, the counterpoise correction (CP) has been proposed to compensate for this error [69]. Indeed, the CP-corrected complexation energy should be calculated as follows:

$$\Delta E^{CP} = E(X - H \cdots Y) - [E(X - H)_{X-H\cdots\{Y\}} - E(Y)_{\{X-H\}\cdots Y}] \quad (2)$$

Now, the energy of each subunit should be calculated in the presence of all the basis functions used in the calculations of X—H···Y. The difference between Eqs. (1) and (2) gives one measure of BSSE.

Making use of the optimization algorithms, it is possible to determine the force field for nuclear displacements of the H-bonded system from the equilibrium geometry, leading directly to the evaluation of its vibrational spectrum. Thus, with the frequencies of the normal modes, one obtains the zero-point vibrational energy (ZPVE) as well as thermodynamic quantities related to the formation of a H-bond [52]. One of the most noticeable characteristics in the vibrational spectrum appears in the band corresponding to the stretch of the X—H bond. Normally, this mode shifts to lower frequency and is intensified so that it is possible to establish a correlation between the amount of the red shift and the strength of the H-bond [59]. Most importantly, the computed vibrational spectra can be compared directly with available Raman and infrared experiments.

2.2. COOPERATIVE EFFECTS AND MANY-BODY INTERACTIONS

Aggregation phenomena involving many molecules are known as nonadditivity or cooperativity [52, 70, 71]. These are of particular interest in H-bonded systems because of the diffuse nature and high polarizability of the hydrogen and lone-pair electron densities [72]. An important type of cooperative effects occurs when the species involved possess both acceptor and donor properties, forming large chains or cycles. This effect is commonly observed in water or HCN clusters [19, 52, 53, 73]. Notwithstanding, multiple H-bonds are not always strongly interacting as in the case of chains or cycles. For example, when a H-bond is

formed between two water molecules, the one donating the hydrogen atom increases the ability of accepting a new H-bond. In contrast, the proton acceptor molecule reduces the ability of accepting a new H-bond, although it becomes a better proton donor. The electron redistribution thus results in both the cooperativity (e.g., accepting one H-bond favors the donation of another) and anticooperativity (e.g., accepting one H-bond unfavors acceptance of another) in hydrogen bonding networks.

To evaluate the cooperative effects quantitatively, it is usual decomposing the total interaction energy of a cluster with N interacting molecules into a sum of multiple-body terms, according to the partition scheme [19, 74]:

$$\Delta E_N = \sum_{i=1}^{N-1} \sum_{j>i}^{N} U_2(i,j) + \sum_{i=1}^{N-2} \sum_{j>i}^{N-1} \sum_{k>j}^{N} U_3(i,j,k) + \cdots \tag{3}$$

The terms $U_K(K = 2 - N)$ in Eq. (3) correspond to the two- through N-body single contributions in the total interaction energy of the aggregate. The multiple-body terms are recursively obtained from the total energy of singlets, $E_1(i)$, doublets, $E_2(i,j)$, triplets, $E_3(i,j,k)$, etc., defined as follows:

$$
\begin{aligned}
U_2(i,j) &= E_2 - [E_1(i) - E_2(j)], \\
U_3(i,j,k) &= E_3(i,j,k) - [U_2(i,j) + U_2(i,k) + U_2(j,k)] \\
&\quad - [E_1(i) + E_1(j) + E_1(k)], \\
U_4(i,j,k,l) &= E_4(i,j,k,l) - [U_3(i,j,k) + U_3(i,j,l) \\
&\quad + U_3(i,k,l) + U_3(j,k,l)] - [U_2(i,j) \\
&\quad + U_2(i,k) + U_2(i,l) + U_2(j,k) + U_2(j,l) \\
&\quad + U_2(k,l)] - [E_1(i) + E_1(j) + E_1(k) + E_1(l)], \\
&\cdots\cdots\cdots
\end{aligned}
\tag{4}
$$

Among the multiple-body terms, the three-body contribution (also denoted as $\Delta E_{3-\text{body}}$) plays an important role in the stabilization of large hydrogen bonded clusters [71]. Furthermore, these interactions are known to affect many properties of H-bonded systems in the condensed phase [75]. While three-body terms are essential to describe cooperative effects, contributions from four-body and higher terms are negligible. In this sense, analytical potentials based on three-body interactions have been developed for describing the dynamics of HF aggregates [76]. Advances in the spectroscopic techniques, which are able to probe small clusters [77], have aided the determi-

nation of three-body effects without the complicating effects of higher orders. The experimental techniques coupled with advances in theoretical treatments moved investigations of many-body interactions to the forefront of the intermolecular interaction research.

2.3. POTENTIAL MODELS FOR LIQUID SIMULATION

Despite the high level of quantum mechanical investigations of molecular clusters—leading to valuable insights into the nature of hydrogen bonding interactions—it is not a simple task to obtain detailed information about the intermolecular potential at all separation distances. Usually, results from these calculations may be factored in a specific partition of the total interaction energy into individual contributions [78, 79]. These are used in formulating suitable expressions for the H-bonding interaction for molecular mechanics calculations [80]. In fact, special potential functions to handle H-bonding interactions can be necessary for the three-dimensional folding of biological macromolecules [81]. On the other hand, in several empirical force field calculations, the hydrogen bonds have been well described by a simple superposition of a Lennard-Jones type potential for nonbonded atoms, and an electrostatic contribution [82], which can be represented by the interaction of partial point charges, such as follows:

$$U_{\alpha\beta}(r_{ij}) = \sum_i^{\text{on }\alpha} \sum_j^{\text{on }\beta} \left\{ 4\varepsilon_{ij} \left[\left(\frac{\sigma_{ij}}{r_{ij}} \right)^{12} - \left(\frac{\sigma_{ij}}{r_{ij}} \right)^6 \right] + \frac{q_i q_j}{r_{ij}} \right\} \tag{5}$$

In molecular liquids and solutions under normal conditions, the nonadditivity problem is commonly bypassed and the total potential energy of N interacting molecules is represented as a sum of two-body terms, so-called effective pair interactions. Such effective potentials have been proposed for several substances by atomistic simulations of liquid-state properties [83, 84]. It is clear that attempts to model solvation process accurately should include three-body contributions. However, it must be emphasized that effective potentials have folded into them various interaction effects, such as polarization of the surrounding solvent molecules, nonrigidity of solutes, anisotropic interactions, etc. Therefore, no explicit

hydrogen bond term is included because the Coulomb and Lennard-Jones terms can accurately represent the hydrogen-bonding interactions [82].

A common procedure to identify hydrogen bonds in liquid simulations is through the radial distribution function (RDF). In this case, spherical integration of the first peak of the RDF between the proton acceptor center and the hydrogen atom of the solvent gives the number of H-bonds formed. The difficulty associated with this procedure is that it cannot be assured that all nearest-neighbor structures are indeed related to H-bonds [6, 13, 85]. An efficient and more correct way to extract the H-bonded structures has been presented by Stilinger and Rahman [86, 87] and Mezei and Beveridge [88]. They have discussed the directional and energetic aspects of H-bonds as well as the importance of identifying H-bonds from computer simulation of liquids. Thus, such interactions are indeed better obtained using the geometric and energetic criteria [6, 13, 49, 85].

3. Applications to H-Bonded Systems

3.1. STRUCTURE AND BINDING OF HCN-WATER ISOMERS

The interaction between HCN and water has been studied both experimentally and theoretically [7, 10, 68, 89–94]. Recently, it has been proposed that the isomerization process between HCN and HNC can be catalyzed by water molecules in the interstellar medium [95, 96]. The experimental microwave studies of Fillery-Travis [89] and Gutowsky et al. [90] have identified the 1:1 structure with the oxygen atom of water bonded to the hydrogen atom of HCN; i.e., $H_2O\cdots HCN$. Another 1:1 structure, with the nitrogen atom of HCN H-bonded to one hydrogen

atom of water; i.e., $HCN\cdots H_2O$, has found to be less stable [7, 68]. Heikkilä et al. [92] studied the infrared spectrum of these complexes in low-temperature argon matrices by FTIR technique and calculated the relative stability of the two isomers by using ab initio calculations at the MP2/6-311++G(2d,2p) level.

We have employed high-level ab initio calculations to determine the equilibrium structures, spectroscopic properties, energetics, and cooperative effects of different HCN-water clusters [7, 10]. The stability of the 1:1 structures obtained with different methods is presented in Table I. It is shown that $HCN\cdots H_2O$ is less bound than $(HCN)_2$, whereas $H_2O\cdots HCN$ is more bound than $(HCN)_2$. In all considered methods given in Table I, we find the following stability order: $HCN\cdots H_2O < HCN\cdots HCN < H_2O\cdots HCN$. This relative stability is very important in determining the precursor of long chains and also the relative abundance of the two species. This is of further interest in the interstellar medium and in comets, where the astrophysical properties may provide important clues regarding the formation of complex organic molecules.

In a systematic study, using the aug-cc-pVXZ basis set series with X = D,T,Q, and extending the results to the infinite basis limit, Malaspina et al. [68] have corroborated that $H_2O\cdots HCN$ is more stable than $HCN\cdots H_2O$ by ~6 kJ/mol. By including the extrapolated value, the MP2 method gives binding energies of 17.45 and 12.38 kJ/mol for $H_2O\cdots HCN$ and $HCN\cdots H_2O$ complexes, respectively, as the differences in zero-point vibrational energies and the correction for BSSE are considered. Heikkilä et al. [92] have obtained these binding energies, without including ZPE, as 19.66 and 15.31 kJ/mol using the MP2/6-311++G(2d,2p) level of theory, which are in accordance with our previous results (Table I).

TABLE I _____

Computed binding energies (in kJ/mol) with counterpoise corrections of water-HCN complexes in comparison with the HCN dimer.

Binding energy	$H_2O\cdots HCN$	$HCN\cdots H_2O$	$(HCN)_2$
MP2/6-311++G(d,p)	19.67	14.80	17.72
MP4//MP2/6-311++G(d,p)	19.07	14.17	17.15
CCSD//MP2/6-311++G(d,p)	19.10	13.46	16.62
CCSD(T)//MP2/6-311++G(d,p)	19.16	13.96	16.81
B3LYP/6-311++G(d,p)	22.27	15.13	17.96
MP2/6-311++G(3df,2p) [94]	20.34	15.79	19.21
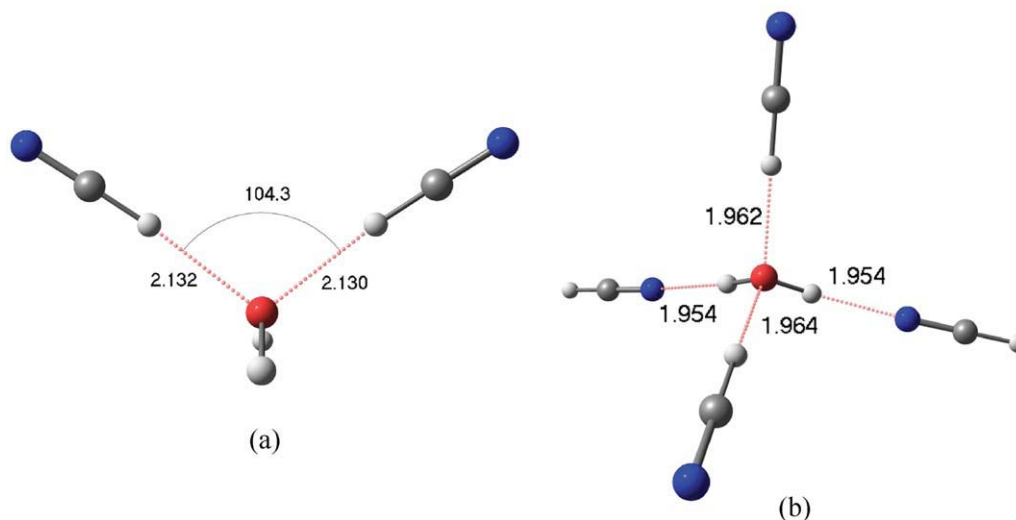
FIGURE 1. Optimized structures of (a) $H_2O\cdots(HCN)_2$ and (b) $(HCN)_2\cdots H_2O\cdots(HCN)_2$ with PW91/aug-cc-pVTZ level of DFT. In (a), the water molecule is oriented such that the hydrogen bonds form approximately in the tetrahedral directions, i.e., in the lone pair directions. In (b), the water molecule forms an extended tetrahedral structure, acting as both proton acceptor and proton donor. H-bond distances are given in Å and angles in degrees. [Color figure can be viewed in the online issue, which is available at wileyonlinelibrary.com.]

However, in Ref. 68, Malaspina et al. have determined that under typical conditions of supersonic expansion experiments ($T < 150$ K), $H_2O\cdots HCN$ is essentially the dominant isomer.

3.2. SUPRAMOLECULAR HCN-WATER CLUSTERS

Here, it is important to mention that HCN-water complexes are expected to form supramolecular structures, such as those formed with one water molecule H-bonded to two HCN molecules or one water molecule H-bonded to four HCN molecules (Fig. 1). These complexes have been obtained as true minima within DFT (PW91/aug-cc-pVTZ), presenting intense intermolecular vibrational modes in the infrared spectra. Furthermore, large three-dimensional HCN structures oriented by a single water molecule are expected to exist in special conditions (Rivelino and Canuto, in preparation). It is interesting to note that $H_2O\cdots(HCN)_2$ is an example of negative cooperativity [52], where the oxygen atom serves as proton acceptor to both HCN molecules. However, it forms a highly stable structure ($\sim$24 kJ/mol, after ZPVE correction) and is also capable to donate both hydrogen atoms, forming $(HCN)_2\cdots H_2O\cdots(HCN)_2$ ($\sim$80 kJ/mol, after ZPVE correction). As both water and HCN are common elements in planetary environments, the relative abundance of

the isomeric H-bonded water-cyanide clusters can play an important role for the formation of structures like $(HCN)_N\cdots H_2O\cdots(HCN)_N$.

Table II displays some important vibrational modes that occurs in these supramolecular complexes. Particularly, in the case of $H_2O\cdots(HCN)_2$, it is noticed librations (restricted rotations; i.e., rocking motions) of the water molecule raging from 252 to 343 cm^{-1}. These librations are consequences of the restrictions imposed by hydrogen bonding, and their combinations with other vibrational motions are responsible for more complex infrared and Raman spectra of liquid water and ice than the vapor [99]. Indeed, in the case of $(HCN)_2\cdots H_2O\cdots(HCN)_2$, we observe that the librations are shifted to higher wavenumber region; i.e., 533 to 649 cm^{-1}. Moreover, with the complete spatial confinement of water translational vibrations of its center of mass are observed in the 181–207 cm^{-1} (5.4–6.2 THz) range. These involve H-bonded network movements along linear or near-linear hydrogen bonds and show a resemblance with the condensed phase of water [100]. Some bending vibrations of the hydrogen bonds also occur, due to out of alignment translations relative to O—H$\cdots$N (70–104 cm^{-1}) and C—H$\cdots$O (138–156 cm^{-1}) H-bonds.

Large red shifts are observed in the C—H stretch of $H_2O\cdots(HCN)_2$, i.e., 124 and 110 cm^{-1} for the asymmetric and symmetric combinations,

TABLE II

Computed vibrational modes (in cm^{-1}) of the
$H_2O\cdots(HCN)_2$ complex with PW91/aug-cc-pVTZ.

Modes	$H_2O\cdots(HCN)_2$	H_2O	HCN
H_2O libration	252	—	—
H_2O libration	296	—	—
H_2O libration	343	—	—
HCN bend	—	—	724 (712)
HCN bend[a] (asym.)	806	—	—
HCN bend[a] (sym.)	816	—	—
HCN bend[b] (sym.)	828	—	—
HCN bend[b] (asym.)	831	—	—
H_2O bend	1600	1595 (1590)	—
CN stretch (asym.)	2111	—	—
CN stretch (sym.)	2114	—	—
CN stretch	—	—	2124 (2097)
CH stretch (asym.)	3247	—	—
CH stretch (sym.)	3261	—	—
CH stretch	—	—	3371 (3311)
H_2O stretch (sym.)	3687	—	—
H_2O stretch (asym.)	3783	—	—
H_2O stretch (sym.)	—	3705 (3638)	—
H_2O stretch (asym.)	—	3809 (3733)	—

Values in parenthesis correspond to the experimental data
[97, 98].
[a] In-plane N—H.
[b] Out-of-plane N—H.

respectively. These shifts increase to 272 and
248 cm^{-1} in $(HCN)_2\cdots H_2O\cdots(HCN)_2$. Interestingly,
the O—H symmetric stretch of H_2O is signifi-
cantly reduced by 199 cm^{-1}, whereas the asym-
metric mode is reduced by 244 cm^{-1}, upon the
$(HCN)_2\cdots H_2O\cdots(HCN)_2$ formation. As seen,
increased strength of hydrogen bonding typically
shifts the stretch vibration to lower frequencies
with greatly increased intensity in the infrared.
Although the present results indicate some coop-
erative effects in these structures, regions of the
potential surface associated with intermolecular
coordinates may be quite flat, so that distortions
away from the idealized structures (those with
directed lone pairs at the proton acceptor sites
and linear X—H⋯Y H-bonds) are very common
(Fig. 1).

3.3. HCN LINEAR CHAINS

Structures and vibrational spectra of pure HCN
clusters have been extensively investigated in the
last decades [73], and continue to be an issue of
great interest for studies of hydrogen bonding
interactions [19, 52]. With the advances in the ex-

perimental techniques [101], optically selected
mass spectra combined with infrared spectrum
have shown vibrational bands associated with
$(HCN)_N$ complexes ($N = 2$–5) formed in helium
nanodroplets. On the theoretical side, recent stud-
ies of the interaction energies and NMR indirect
nuclear spin–spin coupling constants in linear HCN
chains have been performed by Provasi et al. [102]
with the theory of polarization propagators. Further
theoretical studies of neutral and charged HCN
clusters have been carried out by Sánchez et al.
[103] by using DFT and MP2 methods.

Spectroscopic and geometric parameters of
HCN have been discussed by us [104] using
highly correlated levels of theory. Later, we have
quantified multiple-body interaction terms of H-
bonded HCN strings by performing a systemati-
cal analysis within MBPT/CC methods [19].
Because of the possibility of resonance with the
H—C$^+$::N$^-$: structure, involving a positive formal
charge on the carbon atom, the H-bonds are suffi-
ciently strong to stabilize linear polymers of
HCN, even in condensed phase. However, it is
well accepted that hydrogen bond formation in
HCN clusters possesses a cooperative character
[52]. This phenomenon is associated with the non-
additive terms, such as U_3, U_4, etc., given by Eq.
(4), which provide the many-body effects in the
total H-bonding interaction.

A multiple-body decomposition of small chains
($N = 1$–5) is shown in Table III. As seen, these
terms show a significant dependence on the clus-
ter size. For instance, in the case of $(HCN)_4$, we
have obtained contributions of −56.54, −5.80, and
−0.25 kJ/mol for the total two-, three-, and four-
body terms, respectively. The three-body contri-
bution gives about 9% of the total interaction
energy, as normally expected for these types of
systems. The four-body contribution, however, is
considerably smaller; being less than 1% of the
total interaction. The higher-order terms are small
but not totally negligible for very larger clusters.
In the case of $(HCN)_5$, the total four-body contri-
bution is −0.63 kJ/mol, whereas the five-body
contribution is only −0.02 kJ/mol. Now, the
three-body is 11%, whereas the four-body contri-
bution continues to be less than 1%, of the total
hydrogen bonding interaction. The five-body term
gives a negligible contribution to the total interac-
tion of the pentamer.

In our study of Ref. [19], we have employed
MBPT/CC theories to quantify the magnitudes
and high-order correlation effects of two- through

TABLE III

Calculated interaction energies and total multiple-body analysis (kJ/mol)[a] of linear $(HCN)_N$ strings using the MP2/6-311++G(d,p) level of theory.

N	ΔE_N	$\Delta E_{2\text{-body}}$	$\Delta E_{3\text{-body}}$	$\Delta E_{4\text{-body}}$	$\Delta E_{5\text{-body}}$	Cooperativity[b]
2	−17.72	−17.72	—	—	—	—
3	−39.47	−36.98	−2.48	—	—	−4.29
4	−62.59	−56.54	−5.80	−0.25	—	−4.72
5	−86.29	−76.16	−9.48	−0.63	−0.02	−5.14

[a] CP corrections are included.
[b] $[\Delta E_N - (N-1)\Delta E_2]/N - 2$ (see details in Ref. [19]).

five-body terms in the total interaction energy of HCN linear chains. Geometries were optimized with MP2/6-311++G(d,p) and binding energies were calculated up to the CCSD(T) level. We have noticed that higher-order electron correlation does not give a sizable contribution to the strength of the H-bond interactions, which is mainly dominated by electrostatic contribution, as expected for highly polar systems [27]. In Figure 2, we display the calculated dipole moment per molecule as a function of the number of monomers. Extrapolation to large N values shows that the induced dipole moment is 3.87 D; i.e., there is essentially an increase of ~30% relative to the isolated dipole moment of the HCN molecule. In fact, an approach based on electrostatic inductions can be rather reliable for a quantitative description of the cooperative effects in linear HCN clusters.
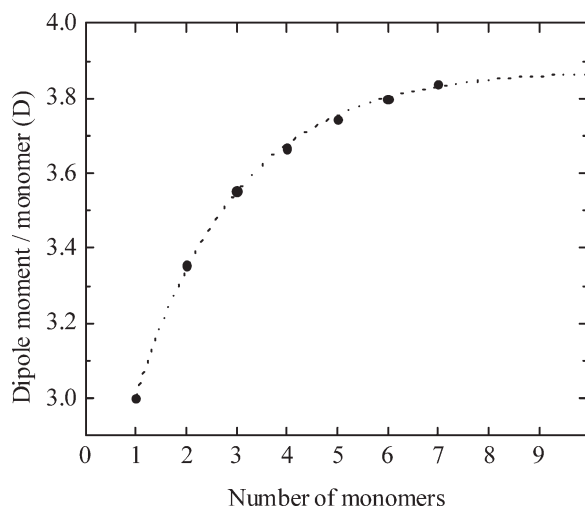

FIGURE 2. Calculated linear polarization of a HCN chain at the MP2//6-311++G(d,p) level. Extrapolation of the average dipole moment indicates that cooperativity effects are dominated by induction effects.

3.4. LEWIS ACID-BASE H-BONDED COMPLEXES

Beyond a typical hydrogen bond, some complexes can form special types of intermolecular interactions, e.g., Lewis acid–base interactions [34]. Recently, evidence for these cooperative interactions in the acetaldehyde-CO_2 complex has been provided by Raman spectroscopy [105]. Also, ab initio calculations of CO_2 complexes with simple model carbonyl compounds identified the possibility of a weaker C—H···O interaction that acts cooperatively with the Lewis acid–base interaction having hydrogen atoms attached to the α-carbon or the carbonyl [106]. However, as noticed by Kryachko, there are still problems that are related to these systems and that are awaiting their complete understanding [54]. In particular, other small molecules possessing electron deficient carbon atoms, e.g., HCN and FCN, are also candidates for working as Lewis acids in the presence of carbonyl compounds [34].

The optimized structural arrangements of the $HCHO\cdots CO_2$, $HCHO\cdots HCN$, and $HCHO\cdots FCN$ complexes are shown in Figure 3. These complexes are supposed to be mostly stabilized by Lewis acid–base interactions, involving the carbonyl oxygen atom in formaldehyde and the electron-deficient carbon atom in CO_2, HCN, or FCN. As suggested in Figure 3, it is possible to identify weak H-bond interactions of the type C—H···Y (Y = O, N) shared with the aldehydic proton. Similarly, in the case of HCN, an H-bonding interaction of the type C—H···O is also expected to be formed with the carbonyl oxygen atom. Some important parameters and properties of these complexes are summarized in Table IV. A typical observation related to the formation of these complexes is that the CO_2, HCN, and FCN molecules become slightly bent after bound,
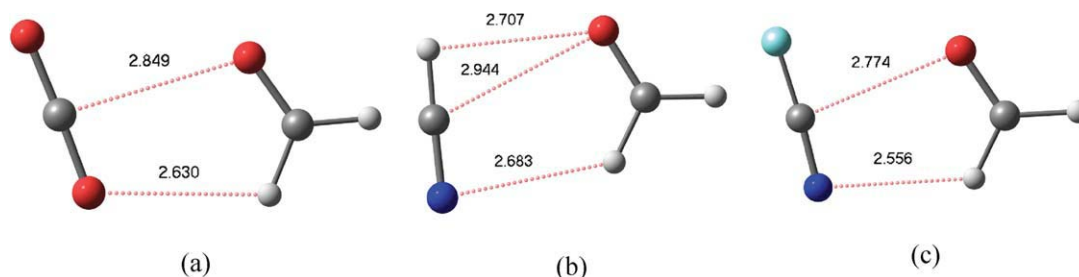
FIGURE 3. Lewis acid–base complexes of formaldehyde with (a) CO_2, (b) HCN, and (c) FCN. Distances are given in Å. [Color figure can be viewed in the online issue, which is available at wileyonlinelibrary.com.]

leading to a splitting in the v_2 vibrational mode of the linear molecules [34, 105, 106].

As reported in Table IV, the degeneracy of v_2 is lifted in the complexes. This seems to be directly connected with the interaction between the electron-deficient carbon (the Lewis acid) of CO_2, HCN, or FCN and the carbonyl oxygen of HCHO. The largest calculated splitting was obtained for the HCHO⋯HCN complex (48 cm^{-1}), whereas HCHO⋯CO_2 and HCHO⋯FCN gave a very similar splitting of $\sim$16 cm^{-1}, although these latter complexes presented very different stabilizations ($\sim$6 and 11 kJ/mol, respectively). In addition to the Lewis acid–base interaction, the blue shifts calculated for the symmetric stretch (v_s) of C—H in HCHO bonded to CO_2, HCN, and FCN were, respectively, 11, 14, and 16 cm^{-1}, indicating the presence of weak, but coop-

erative, H bonds. Also, a small blue sift of only 2 cm^{-1} was obtained for the NC—H symmetric stretch in HCHO⋯HCN. In summary, this study has shown that HCN and FCN form stable complexes like the Lewis acid–base HCHO⋯CO_2 complex, opening important perspective to understand the interactions between HCN and carbonyl groups.

3.5. CONFORMATIONAL ANALYSIS OF FURFURAL

Having discussed the main structural and energetic features behind a H-bond in molecular aggregates, it is worthwhile now to go beyond a static structure (in its equilibrium geometry) to a solute embedded in a solvent, where temperature effects are included. As an interesting example,

TABLE IV

Calculated properties of the weakly bound formaldehyde complexes with CO_2, HCN, and FCN at the MP2(Full)/aug-cc-pVDZ level.

Properties	HCHO⋯CO_2	HCHO⋯HCN	HCHO⋯FCN
Bond lengths (Å)			
C–H[a]	1.109	1.109	1.109
H⋯Y	2.630	2.683	2.556
O⋯C	2.849	2.944	2.774
Bond angles (°)			
OCH	121.4	121.5	121.2
C–H⋯Y	110.8	127.5	118.7
C–H⋯O	—	91.8	—
Binding energy[b] (kJ/mol)	6.32	11.05	11.42
v_2 splitting (cm^{-1})	16	48	16
Vibrational shifts (cm^{-1})			
v_s	11	14	16
C=O stretch	−4	−6	−9

[a] The C–H distance in the isolated species is 1.111 Å.
[b] Corrected for BSSE, ZPVE, and geometric deformations (see details in Ref. [34]).
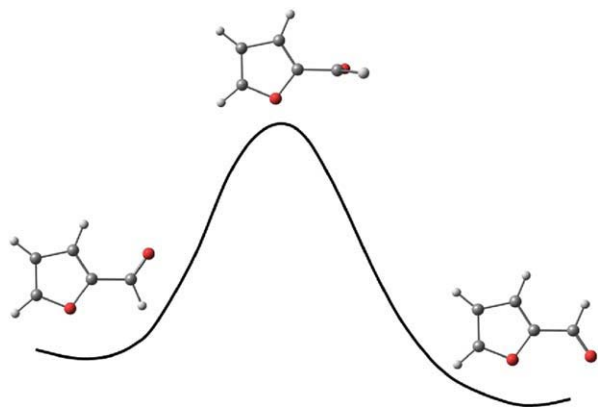
FIGURE 4. Illustration of the conformational equilibrium of furfural. The OO-*trans* form is more stable in the vapor, whereas the OO-*cis* form is more stable in polar solvents. [Color figure can be viewed in the online issue, which is available at wileyonlinelibrary.com.]

the conformational equilibrium of furfural (Fig. 4) in protic solvents is examined here via atomistic simulations [13, 26], with the intermolecular interactions described by Eq. (5). Since the early infrared and Raman studies by Allen and Bernstein [107], this mechanism has continued to fascinate chemists. Recently, rotational barrier and thermodynamic parameters of furfural in solvents of different polarities have been investigated based on DFT calculations [108]. All these studies have shown that in the gas phase, the OO-*trans* conformer is always more stable, but increasing the polarity of the solvent leads the OO-*cis* conformer to become more stable [109].

Baldridge et al. [110] showed that the conformer with larger dipole moment, OO-*cis*, pre-vails in solvents with dielectric constants higher than 5. However, the stability between both conformers does not obey a simple relationship with the dielectric constant. This, of course, indicates that the solvent effects are more complex than could be inferred by a simple reaction field [26]. NMR measurements [111] have been used to determine the thermodynamic parameters for the rotation of the carbonyl group in furfural in toluene, acetone, and methanol. For instance, important entropy effects were observed in nonprotic solvents, e.g., toluene and acetone, and no effects in protic solvents such as methanol.

The statistical analysis from atomistic Monte Carlo (MC) simulations of the hydrogen bond formation of furfural in water and chloroform (a weaker protic solvent than water) is presented in Table V. In principle, it is expected that in protic solvents like water the H-bonds formed with the oxygen atoms of the furfural molecule could favor a particular conformation to the detriment of another. To understand the specific role of the solute–solvent interactions during the internal rotation, we have performed a detailed structural investigation of the H-bonding water [13]. Each H-bond formed between furfural and the solvent is defined using the geometric and energetic criteria [86–88]; these are $R_{OX} \leq 3.7$ Å, $\theta_{OXH} \leq 36°$, and positive binding energies. Table V summarizes results corresponding to the three most representative conformers (OO-*cis*, transition state (TS), and OO-*trans*) of furfural in water and chloroform. This analysis provides a microscopic description of the specific interaction involving the proton acceptor furfural and the proton donor water or chloroform during the cis–trans interconversion.

TABLE V

Calculated averages properties[a] of H-bonding formation[b] in furfural in solutions.

H_2O	# H-Bond	O···X	O···X–H	$-\Delta E$/H-bond
OO-*cis*	0.97	3.03 ± 0.23	19.5 ± 8.0	14.06 ± 2.93
OO-TS	0.84	2.98 ± 0.23	20.8 ± 8.0	12.89 ± 2.51
OO-*trans*	1.13	2.95 ± 0.23	16.5 ± 8.0	12.89 ± 2.93
$CHCl_3$				
OO-*cis*	1.07	3.26 ± 0.23	21.7 ± 8.0	13.64 ± 2.93
OO-TS	0.97	3.24 ± 0.23	20.9 ± 8.0	13.43 ± 2.09
OO-*trans*	0.92	3.27 ± 0.23	20.7 ± 8.0	13.35 ± 2.51

[a] Distances in Å, angles in degree, and binding energies in kJ/mol.
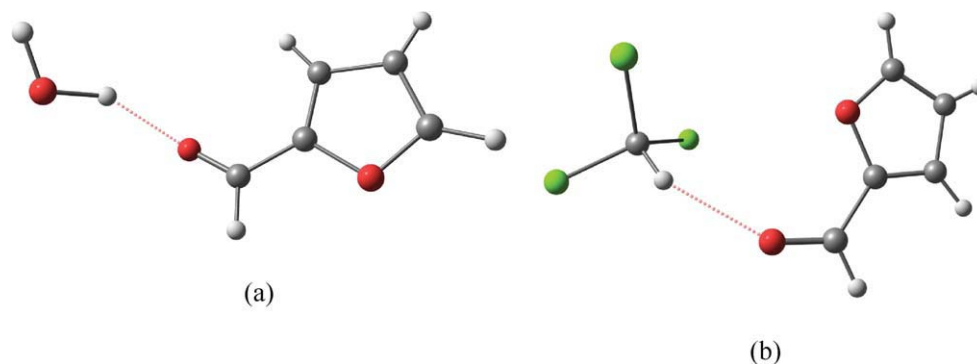[b] X = C (in chloroform) or O (in water).

FIGURE 5. Hydrogen bonding interactions between furfural and (a) water and (b) chloroform obtained from MC simulations under ambient conditions. [Color figure can be viewed in the online issue, which is available at wileyonlinelibrary.com.]

In the aqueous solution, we have calculated for the OO-*cis* that 23% of the configurations make no H-bond, 58% make one, 17% make two, and 2% make even three H-bonds. Then, out of the 60 MC configurations selected, there exist 58 H-bonds in the OO-*cis* conformer, making therefore, 0.97 H-bond on average. This is the statistics of the hydrogen bonding interactions for the solution of furfural in water. In fact, most of the H-bonds have the carbonyl oxygen as the proton acceptor. Similar results are obtained for the OO-*trans* conformer and transition state, with an average number of 1.13 hydrogen bonds in the first case and 0.84 for the second one. Also, a similar statistics is obtained in chloroform. In Figure 5, it is shown two types of common H-bonds formed with arbitrary conformers of furfural in both solvents.

As noted in Table V, similar H-bonding patterns have been obtained dissolving furfural in water or chloroform. The average number and the strength of hydrogen bonds formed between the solute and the solvent are essentially constant along the internal rotation, which gives no meaningful contribution to the activation entropy. These results are in agreement with previous observations of the investigation of furfural in methanol by Bain and Hazendonk [111]. Thus, atomistic MC simulations have demonstrated that the hydrogen bonding patterns along the rotational equilibrium are very similar. The number of the hydrogen bonds formed and the binding energies change slightly during the internal rotation of the carbonyl group of furfural. This suggests that the hydrogen bonding interactions are not preferentially formed with a particular conformer.

4. Concluding Remarks

This article revisited important topics related to the hydrogen bonding phenomenon, which can be treated by using high-level quantum mechanical calculations or atomistic computer simulations. Some methodological aspects and applications of hydrogen bonding interactions in molecular aggregates and liquid solutions were discussed. In particular, issues that have been research interest of Professor Canuto and his collaborators were briefly reviewed [5–33, 104]. Moreover, new insights into the fundamental nature of the H-bonds in molecular complexes were presented [34, 35] (Rivelino and Canuto, in preparation).

The recent progress that has been made in ab initio electronic structure calculations has permitted high-level investigations to be performed on hydrogen bonding interactions in clusters and extend systems. These studies have produced structures and binding energies of accuracy comparable to that obtained experimentally. Furthermore, they have provided insight into other properties of H-bonded complexes, resulting in a deep understanding of the H-bonding interaction phenomenon. Importantly, advances in experiments have contributed greatly to probe this unique intermolecular interaction.

There are, however, many important problems that remain to be investigated, including hydrogen bonding in associated liquids [44, 112], quantum effects on the proton transfer of hydrogen bonded systems [44, 113], effects of hydrogen bonds in large biochemical structures, which has reveled important cooperative patterns [114], and hydrogen bonding interactions in solvated nanostructures

and supramolecular assembled nanocomposites, such as fullerene derivatives [50, 51, 115].

ACKNOWLEDGMENT

References

1. Coutinho, K.; Canuto, S. J Mol Struct (THEOCHEM) 1993, 106, 99.

2. Piquini, P.; Fazzio, A.; Canuto, S. Z Phys D 1995, 33, 125.

3. Urahata, S.; Coutinho, K.; Canuto, S. Chem Phys Lett 1997, 274, 269.

4. Cunha, C.; Canuto, S. Phys Lett A 1998, 241, 90.

5. Coutinho, K.; Saavedra, N.; Canuto, S. J Mol Struct (THEOCHEM) 1999, 466, 69.

6. Canuto, S.; Coutinho, K. Int J Quantum Chem 2000, 77, 192.

7. Rivelino, R.; Canuto, S. Chem Phys Lett 2000, 322, 207.

8. Coutinho, K.; Canuto, S. J Chem Phys 2000, 113, 9132.

9. Rocha, W. R.; De Almeida, K. J.; Coutinho, K.; Canuto, S. Chem Phys Lett 2001, 345, 171.

10. Rivelino, R.; Canuto, S. J Phys Chem A 2001, 105, 11260.

11. Rivelino, R.; Ludwig, V.; Rissi, E.; Canuto, S. J Mol Struct 2002, 615, 257.

12. Quintao, A. D.; Coutinho, K.; Canuto, S. Int J Quantum Chem 2002, 90, 634.

13. Rivelino, R.; Coutinho, K.; Canuto, S. J Phys Chem B 2002, 106, 12317.

14. Fileti, E. E.; Rivelino, R.; Canuto, S. J Phys B At Mol Opt Phys 2003, 36, 399.

15. Guedes, R. C.; Coutinho, K.; Cabral, B. J. C.; Canuto, S.; Correia, C. F.; dos Santos, R. M. B.; Simoes, J. A. M. J Phys Chem A 2003, 107, 9197.

16. Rivelino, R.; Canuto, S. J Phys Chem A 2004, 108, 1601.

17. Fileti, E. E.; Canuto, S. Int J Quantum Chem 2005, 104, 808.

18. Rivelino, R.; Canuto, S. Int J Quantum Chem 2005, 103, 654.

19. Rivelino, R.; Chaudhuri, P.; Canuto, S. J Chem Phys 2003, 118, 10601.

20. Coutinho, K.; Canuto, S. Adv Quantum Chem 1997, 28, 89.

21. Coutinho, K.; De Oliveira, M. J.; Canuto, S. Int J Quantum Chem 1998, 66, 249.

22. Coutinho, K.; Canuto, S.; Zerner, M. C. J Chem Phys 2000, 112, 9874.

23. Rocha, W. R.; Martins, V. M.; Coutinho, K.; Canuto, S. Theor Chim Acc 2002, 108, 31.

24. Canuto, S.; Coutinho, K.; Trzesniak, D. Adv Quantum Chem 2002, 41, 161.

25. Fileti, E. E.; Coutinho, K.; Canuto, S. Adv Quantum Chem 2004, 47, 51.

26. Rivelino, R.; Canuto, S.; Coutinho, K. Braz J Phys 2004, 34, 84.

27. Rivelino, R.; Cabral, B. J. C.; Coutinho, K.; Canuto, S. Chem Phys Lett 2005, 407, 13.

28. Georg, H. C.; Coutinho, K.; Canuto, S. J Chem Phys 2005, 123, 124307.

29. (a) Coutinho, K. PhD Thesis, University of São Paulo, São Paulo, Brazil, 1997; (b) Cunha, C. PhD Thesis, University of São Paulo, São Paulo, Brazil, 1997; (c) Urahata, S. PhD Thesis, University of São Paulo, São Paulo, Brazil, 1999; (d) Serrano, A. PhD Thesis, University of São Paulo, São Paulo, Brazil, 1999; (e) Saavedra, N. PhD Thesis, University of São Paulo, São Paulo, Brazil, 1999; (f) Rivelino, R. PhD Thesis, University of São Paulo, São Paulo, Brazil, 2003; (g) Rissi, E. PhD Thesis, University of São Paulo, São Paulo, Brazil, 2004; (h) Fileti, E. E. PhD Thesis, University of São Paulo, São Paulo, Brazil, 2004; (i) Ludwig, V. PhD Thesis, University of São Paulo, São Paulo, Brazil, 2005; (j) Malaspina, T. PhD Thesis, University of São Paulo, São Paulo, Brazil, 2006.

30. Ludwig, V.; Coutinho, K.; Canuto, S. Phys Chem Chem Phys 2007, 9, 4907.

31. Almeida, T. S.; Coutinho, K.; Cabral, B. J. C.; Canuto, S. J Chem Phys 2008, 128, 014506.

32. Fonseca, T. L.; Georg, H. C.; Coutinho, K.; Canuto, S. J Phys Chem A 2009, 113, 5112.

33. Jaramillo, P.; Coutinho, K.; Canuto, S. J Phys Chem A 2009, 113, 12485.

34. Rivelino, R. J Phys Chem A 2008, 112, 161.

35. de Carvalho, M. F.; Mosquera, R. A.; Rivelino, R. Chem Phys Lett 2007, 445, 117.

36. Pimentel, G. C.; McClellan, A. L. Annu Rev Phys Chem 1971, 22, 347.

37. Zwier, T. S. Annu Rev Phys Chem 1996, 47, 205.

38. Nibbering, E. T. J.; Elsaesser, T. Chem Rev 2004, 104, 1887.

39. Elsaesser, T. Acc Chem Res 2009, 42, 1220.

40. Banno, M.; Ohta, K.; Yamaguchi, S.; Hirai, S.; Tominaga, K. Acc Chem Res 2009, 42, 1259.

41. Liu, Y.; Li, Y. J.; Jiang, L.; Gan, H. Y.; Liu, H. B.; Li, Y. L.; Zhuang, J. P.; Lu, F. S.; Zhu, D. B. J Org Chem 2004, 69, 9049.

42. Keeling, D. L.; Oxtoby, N. S.; Wilson, C.; Humphry, M. J.; Champness, N. R.; Beton, P. H. Nano Lett 2003, 3, 9.

43. Mota, F. B.; Rivelino, R. J Mol Struct (THEOCHEM) 2006, 776, 53.

44. Tuckerman, M. E.; Marx, D.; Parrinello, M. Nature 2002, 417, 925.

45. Prendergast, D.; Grossman, J. C.; Galli, G. J Chem Phys 2005, 123, 014501.

46. Gao, J. L.; Xia, X. F. Science 1992, 258, 631.

47. Röhrig, U. F.; Frank, I.; Hutter, J.; Laio, A.; VandeVondele, J.; Rothlisberger, U. ChemPhysChem 2003, 4, 1177.

48. Mota, F. D.; Rivelino, R. J Phys Chem B 2009, 113, 9489.

49. Coutinho, K.; Rivelino, R.; Georg, H. C.; Canuto, S. In Solvation Effects on Molecules and Biomolecules: Computational Methods and Applications; Canuto, S., Ed.; Springer-Verlag: Berlin, 2008; Chapter 7.

50. Rivelino, R.; Malaspina, T.; Fileti, E. E. Phys Rev A 2009, 79, 013201.

51. Fileti, E. E.; Rivelino, R.; Mota, F. D.; Malaspina, T. Nanotechnology 2008, 19, 365703.

52. Scheiner, S. Hydrogen Bonding. A Theoretical Perspective; Oxford: New York, 1997.

53. Del Bene, J. E. In The Encyclopedia of Computational Chemistry; Schleyer, P. v. R., Allinger, N. L., Clark, T., Gasteiger, J., Kollman, P. A., Schaefer, H. F., III, Schreiner, P. R., Eds.; Wiley: Chichester, 1998; p 1263.

54. Kryacko, E. S. Int J Quantum Chem 2010, 110, 104.

55. Kryachko, E. S. J Mol Struct 2008, 880, 23.

56. Kar, T.; Scheiner, S. J Phys Chem A 2004, 108, 9161.

57. Swamy, K. C. K.; Kumaraswamy, S.; Kommana, P. J Am Chem Soc 2001, 123, 12642.

58. Vargas, R.; Garza, J.; Dixon, D. A.; Hay, B. P. J Am Chem Soc 2000, 122, 4750.

59. Hobza, P.; Havlas, Z. Chem Rev 2000, 100, 4253.

60. Bartlett, R. J. Annu Rev Phys Chem 1981, 32, 359.

61. Binkley, J. S.; Pople, J. A. Int J Quantum Chem 1975, 9, 229.

62. Arey, J. S.; Aeberhard, P. C.; Lin, I. C.; Rothlisberger, U. J Phys Chem B 2009, 113, 4726.

63. Zhao, Y.; Tishchenko, O.; Truhlar, D. G. J Phys Chem A 2005, 109, 19046.

64. Gordon, M. S.; Binkley, J. S.; Pople, J. A.; Pietro, W. J.; Hehre, W. J. J Am Chem Soc 1982, 104, 2797.

65. Frisch, M. J.; Pople, J. A.; Binkley, J. S. J Chem Phys 1984, 80, 3265.

66. Dunning, T. H., Jr. J Chem Phys 1989, 90, 1007.

67. Woon, D. E.; Dunning, T. H., Jr. J Chem Phys 1993, 98, 1358.

68. Malaspina, T.; Fileti, E. E.; Riveros, J. M.; Canuto, S. J Phys Chem A 2006, 110, 10303.

69. Boys, S. F.; Bernardi, F. Mol Phys 1970, 19, 553.

70. Kollman, P. A.; Allen, L. C. Chem Rev 1972, 72, 283.

71. Keutsch, F. N.; Cruzan, J. D.; Saykally, R. J. Chem Rev 2003, 103, 2533.

72. Jeffrey, G. A. An Introduction to Hydrogen Bonding; Oxford: New York, 1997.

73. Karpfen, A. In Molecular Interactions. From van der Waals to Strongly Bound Complexes; Scheiner, S., Ed.; Wiley: Chichester, 1997.

74. Hankins, D.; Moskowitz, J. W.; Stillinger, F. H. J Chem Phys 1970, 53, 4544.

75. Pauling, L. The Nature of the Chemical Bond and the Structure of Molecules and Crystals: An Introduction to Modern Chemistry; Cornell University Press: Ithaca, NY, 1960.

76. Quack, M.; Stohner, J.; Suhm, M. A. J Mol Struct 2001, 599, 381.

77. Keutsch, F. N.; Saykally, R. J. Proc Natl Acad Sci USA 2001, 98, 10533.

78. Kollman, P. A.; Allen, L. C. Theor Chim Acta 1970, 18, 399.

79. Morokuma, K.; Winick, J. R. J Chem Phys 1970, 52, 1301.

80. Lii, J.-H. In The Encyclopedia of Computational Chemistry; Schleyer, P. v. R.; Allinger, N. L.; Clark, T.; Gasteiger, J.; Kollman, P. A.; Schaefer, H. F., III; Schreiner, P. R., Eds.; Wiley: Chichester, 1998; p 1271.

81. Lii, J.-H.; Allinger, N. L. J Phys Org Chem 1994, 7, 591.

82. MacKerell, A. D.; Bashford, D.; Bellot, M.; Dunbrack, R. L.; Evanseck, J. D.; Field, M. J.; Fischer, S.; Gao, J.; Gao, H.; Ha, S.; Joseph-McCarthy, D.; Kuchnir, L.; Kuczera, K.; Lao, F. T. K.; Mattos, C.; Michnick, S.; Ngo, T.; Nguyen, D. T.; Prodhom, B.; Reiher, W. E.; Roux, B.; Schlenkrich, M.; Smith, J. C.; Stote, R.; Straub, J.; Watanabe, M.; Wiorkiewicz-Kuczera, J.; Yin, D.; Karpius, M. J Phys Chem B 1998, 102, 3586.

83. Jorgensen, W. L. J Phys Chem 1986, 90, 6379.

84. Jorgensen, W. L.; Maxwell, D. S.; Tirado-Rives, J. J Am Chem Soc 1996, 118, 11225.

85. Jorgensen, W. L.; Chandrasekhar, J.; Madura, J. D.; Impey, R. W.; Klein, M. L. J Chem Phys 1983, 79, 926.

86. Rahman, A.; Stilinger, F. H. J Chem Phys 1971, 55, 3336.

87. Stilinger, F. H.; Rahman, A. J Chem Phys 1974, 60, 1545.

88. Mezei, M.; Beveridge, D. L. J Chem Phys 1981, 74, 622.

89. Fillery-Travis, A. J.; Legon, A. C.; Willoughby, L. C. Proc R Soc Lond A 1984, 396, 405.

90. Gutowsky, H. S.; Germann, T. C.; Augspurger, J. D.; Dykstra, C. E. J Chem Phys 1992, 96, 5808.

91. Turi, L.; Dannenberg, J. J. J Chem Phys 1993, 97, 7899.

92. Heikkilä, A.; Pettersson, M.; Lundell, J.; Khriachtchev, L.; Rasanen, M. J Phys Chem A 1999, 103, 2945.

93. Muchova. E.; Spirko, V.; Hobza, P.; Nachtigallova, D. Phys Chem Chem Phys 2006, 8, 4866.

94. Li, Q. Z.; Wang, X. L.; Cheng, J. B.; Li, W. Z.; Gong, B. A.; Sun, J. Z. Int J Quantum Chem 2009, 109, 1396.

95. Gardebien, F.; Sevin, A. J Phys Chem A 2003, 107, 3925.

96. Gardebien, F.; Sevin, A. J Phys Chem A 2003, 107, 3935.

97. Harris, D. C.; Bertolucci, M. D. Symmetry and Spectroscopy. An Introduction to Vibrational and Electronic Spectroscopy; Dover: New York, 1989.

98. Bentwood, R. M.; Barnes, A. J.; Orville-Thomas, W. J. J Mol Spectrosc 1980, 84, 391.

99. Gaiduk, V. I.; Vij, J. K. Phys Chem Chem Phys 2001, 3, 5173.

100. Brubach, J.-B.; Mermet, A.; Filabozzi, A.; Gerschel, A.; Roy, P. J Chem Phys 2005, 122, 184509.

101. Choi, M. Y.; Douberly, G. E.; Falconer, T. M.; Lewis, W. K.; Lindsay, C. M.; Merritt, J. M.; Stiles, P. L.; Miller, R. E. Int Rev Phys Chem 2006, 25, 15.

102. Provasi, P. F.; Aucar, G. A.; Sánchez, M.; Alkorta, I.; Elguero, J.; Sauer, S. P. A. J Phys Chem A 2005, 109, 6555.

103. Sánchez, M.; Provasi, P. F.; Aucar, G. A.; Alkorta, I.; Elguero, J. J Phys Chem B 2005, 109, 18189.

104. Rissi, E.; Rivelino, R.; Canuto, S. Int J Quantum Chem 2003, 91, 575.

105. Blatchford, M. A.; Raveendran, P.; Wallen, S. L. J Am Chem Soc 2002, 124, 14818.

106. Raveendran, P.; Wallen, S. L. J Am Chem Soc 2002, 124, 12590.

107. Allen, G.; Bernstein, H. J. Can J Chem 1955, 33, 1055.

108. Ashish, H.; Ramasami, P. Mol Phys 2008, 106, 175.

109. Abraham, R. J.; Bretschneider, E. In Internal Rotation in Molecules; Orville-Thomas, W. J., Ed.; Wiley: New York, 1974; p 481.

110. Baldridge, K. K.; Jonas, V.; Bain, A. D. J Chem Phys 2000, 113, 7519.

111. Bain, A. D.; Hazendonk, P. J Phys Chem 1997, 101, 7182.

112. Boese, A. D.; Chandra, A.; Martin, J. M. L.; Marx, D. J Chem Phys 2004, 119, 5965.

113. Berkelbach, T. C.; Lee, H.; Tuckerman, M. E. Phys Rev Lett 2009, 103, 238302.

114. Pinteala, M.; Dascalu, A.; Ungurenasu, C. Int J Nanomedicine 2009, 4, 193.

115. Ouyang, J.; Zhou, S.; Wang, F.; Goh, S. H. J Phys Chem B 2004, 108, 5937.